

Aberrant DNA methylation characterizes juvenile myelomonocytic leukemia (JMML) with poor outcome

Christiane Olk-Batz^{1,2}, Anna R. Poetsch³, Peter Nöllke¹, Rainer Claus³, Manuela Zucknick⁴, Inga Sandrock¹, Tania Witte³, Brigitte Strahm¹, Henrik Hasle⁵, Marco Zecca⁶, Jan Starý⁷, Eva Bergstraesser⁸, Barbara De Moerloose⁹, Monika Trebo¹⁰, Marry M. van den Heuvel-Eibrink¹¹, Dorota Wojcik¹², Franco Locatelli¹³, Christoph Plass³, Charlotte M. Niemeyer¹ and Christian Flotho^{1*}; on behalf of the European Working Group of Myelodysplastic Syndromes in Childhood (EWOG-MDS)

¹Dept. of Pediatrics and Adolescent Medicine, University Medical Center, Freiburg, Germany; ²Dept. of Biology, University of Freiburg, Freiburg, Germany; Divisions of ³Epigenomics and Cancer Risk Factors and ⁴Biostatistics, German Cancer Research Center, Heidelberg, Germany; ⁵Dept. of Pediatrics, Aarhus University Hospital Skejby, Aarhus, Denmark; ⁶Pediatric Hematology-Oncology, Fondazione IRCCS Policlinico San Matteo, Pavia, Italy; ⁷Dept. of Pediatric Hematology and Oncology, Charles University Prague, Prague, Czech Republic; and Czech Pediatric Hematology Working Group (CPH), Czech Republic; ⁸Dept. of Pediatric Hematology-Oncology, University Children's Hospital, Zürich, Switzerland; ⁹Dept. of Pediatric Hematology-Oncology, Ghent University Hospital, Ghent, Belgium; ¹⁰Dept. of Pediatrics, St. Anna Children's Hospital, Vienna, Austria; ¹¹Dept. of Pediatric Oncology/Hematology, Erasmus Medical Center, Rotterdam, The Netherlands; Dutch Childhood Oncology Group, The Netherlands; ¹²Dept. of Pediatric Hematology-Oncology, Wroclaw Medical University, Wroclaw, Poland; ¹³Dept. of Pediatric

Hematology-Oncology, IRCCS Ospedale Bambino Gesù, Roma, University of Pavia,
Italy

*Correspondence: Dr. Christian Flotho, Pädiatrische Hämatologie und Onkologie,
Zentrum für Kinder- und Jugendmedizin der Universität Freiburg, Mathildenstr. 1,
79106 Freiburg, Germany.

E-mail: christian.flotho@uniklinik-freiburg.de

Phone: +49 761 270 4506

Fax: +49761 270 4518

Running Head: DNA Methylation in JMML

Type of Submission: Regular Article

Section Designation: Myeloid Neoplasia

Word Count Abstract: 196

Word Count Text: 4166

Reference Count: 40

Tables: 2

Figures: 5

Supplemental Tables: 4

Supplemental Figures: 4

Abstract

Aberrant DNA methylation contributes to the malignant phenotype in cancer including myeloid leukemia. We hypothesized that CpG island hypermethylation also occurs in juvenile myelomonocytic leukemia (JMML) and asked whether it is associated with clinical, hematologic or prognostic features. Based on quantitative measurements of DNA methylation in 127 JMML cases using mass spectrometry (MassARRAY), we identified four gene CpG islands with frequent hypermethylation: *BMP4* (36% of patients), *CALCA* (54%), *CDKN2B* (22%), and *RARB* (13%). Hypermethylation was significantly associated with poor prognosis: when the methylation data was transformed into prognostic scores using a LASSO Cox regression model, the 5-year overall survival was 0.41 for patients in the top tertile of scores versus 0.72 in the lowest score tertile ($p=0.002$). Among patients given allogeneic hematopoietic stem cell transplantation, the 5-year cumulative incidence of relapse was 0.52 in the highest versus 0.10 in the lowest score tertile ($p=0.007$). In multivariate models, DNA methylation retained prognostic value independently of other clinical risk factors. Longitudinal analyses indicated that some cases acquired a more extensively methylated phenotype at relapse. In conclusion, our data suggest that a high-methylation phenotype characterizes an aggressive biologic variant of JMML and is an important molecular predictor of outcome.

Introduction

Epigenetic changes, defined as mitotically heritable changes in gene expression without DNA sequence alterations, accompany the development and progression of malignant disease. A hallmark of the molecular phenotype of malignant transformation is global DNA hypomethylation coupled with regional DNA hypermethylation. Hypermethylation occurs in a tumor-specific pattern at CpG island sequences representing CG-rich regions frequently located at the 5' end of coding genes. These changes can affect gene promoter functionality, resulting in stable gene silencing.¹ CpG island hypermethylation is found in virtually all kinds of cancer, including myeloproliferative neoplasms (MPN), myelodysplastic syndrome (MDS) and myeloid leukemia.²

Juvenile myelomonocytic leukemia (JMML) is an aggressive MPN of early childhood. An important feature of the molecular pathophysiology of JMML is the deregulation of the Ras signal transduction pathway, caused by mutations in the *PTPN11*, *NRAS*, *KRAS*, *CBL* or *NF1* genes.³⁻⁵ The clinical risk assessment in JMML involves age at diagnosis, thrombocytopenia and fetal hemoglobin (HbF) as main prognostic variables.⁶ However, the molecular basis of the prognostic diversity in JMML remains barely understood, and it is yet unclear if and how specific Ras pathway lesions determine the clinical course.

Available literature on aberrant CpG island methylation in JMML is limited to a few genes in small series of patients, including the *CDKN2A* (hypermethylation reported in 0/18 cases),⁷ *CDKN2B* (3/18 cases),⁷ *RASSF1A* (1/5 cases),⁸ *PTPN6* (0/5 cases),⁸ *SOCS1* (0/5 cases)⁸ and *PTEN* (23/30 in one series but 0/90 in another)^{9,10} genes. In this study, we investigated the DNA methylation status of 14 gene CpG islands in a large cohort of JMML patients and asked whether aberrant

methylation is associated with clinical, hematologic or prognostic features of the disease. We report that the presence or absence of hypermethylation characterizes subsets of the disease with distinct clinical behavior and that CpG island hypermethylation is an important molecular marker of prognosis in JMML.

Material and Methods

Patient samples. Clinical samples from 127 children with JMML were collected in the context of the European Working Group on MDS in Childhood (EWOG-MDS) studies 98 and 2006 (registered with the United States National Institute of Health, clinicaltrials.gov identifiers: NCT00047268 and NCT00662090), after obtaining informed consent from parents or legal guardians and approval from institutional review committees at each participating center. Diagnostic samples included bone marrow (BM) in 70 cases and peripheral blood (PB) in 57 cases. Hematopoietic spleen cells were obtained from organs removed for clinical indication in 2 cases and were used for flow cytometry cell sorting experiments. Each BM/PB/spleen cell sample was separated into mononuclear cells (MNC) and granulocytes by density gradient centrifugation. Unfractionated PB leukocytes from 15 healthy individuals were used as controls.

Nucleic acid extraction. Genomic DNA was isolated using the Puregene (Qiagen, Hilden, Germany) or Transfast (Peqlab, Erlangen, Germany) kits. Total RNA was isolated from MNC using the Trizol reagent (Invitrogen, Karlsruhe, Germany).

Bisulfite conversion and bisulfite sequencing. 500ng of genomic DNA was bisulfite-modified using the EZ Methylation Gold kit (Zymo Research, Orange, CA, USA). Primers used for subsequent amplification are listed in Supplemental

Table S1. Polymerase chain reaction products were either gel-purified using GFX columns (GE Healthcare, München, Germany) prior to ligation or directly ligated into the pCR 2.1 vector (Invitrogen). Six to eight clones per sample were sequenced using BigDye terminator chemistry (Applied Biosystems, Darmstadt, Germany) and capillary electrophoresis. Complete bisulfite modification was confirmed by sequence analysis.

MassARRAY. Quantitative DNA methylation analysis at single CpG units was performed using MassARRAY EpiTyper as previously described.¹¹ Briefly, bisulfite-treated genomic DNA was PCR-amplified, *in vitro* transcribed, cleaved by RNase A and subjected to matrix-assisted laser desorption ionisation-time of flight mass spectrometry (Sequenom, Hamburg, Germany). Primer sequences for PCR amplicons in relation to CpG island positions are listed in Supplemental Table S1. Methylation standards (0%, 20%, 40%, 60%, 80% and 100% methylated genomic DNA) and correction algorithms based on custom scripts for the R statistical computing environment were used for data normalization.

Quantitative real-time reverse-transcription PCR. The QuantiTect Reverse Transcription kit (Qiagen) was applied including a procedure to remove genomic DNA. Quantitative PCR was performed on a Mastercycler EP Realplex (Eppendorf, Hamburg, Germany) using ABSolute QPCR SYBR Green reaction mix (Thermo Scientific, Epsom, United Kingdom) and primers listed in Supplemental Table S1. GAPDH was used as internal control. RT-PCR reactions were performed in triplicate, including no-template controls. Relative expression was calculated using the comparative C_T method.

Flow cytometry cell sorting. Cryopreserved spleen MNC were thawed using medium supplemented with 20 U/ml DNase I. Ten μ l CD3-FITC, CD14-PE, CD19-

PE, CD34-PE or CD235a-FITC antibody (BD Biosciences, Erembodegem, Belgium) was added per 10^6 cells. Cells were incubated for 30 minutes, washed twice and sorted on a MoFlo high-speed cell sorter (Dako, Hamburg, Germany). The purity of each fraction was checked and found to be greater than 90%.

Pyrosequencing. Specific long interspersed nuclear element 1 (LINE1) primers (Qiagen) were used for PCR of bisulfite-converted DNA. Biotin labeled PCR products were bound to Streptavidin Sepharose HP (Amersham Biosciences, Uppsala, Sweden). The sepharose beads were purified, washed, denatured in 0.2 M NaOH, and washed again. Pyrosequencing was performed on a PyroMark Q96 MD (Qiagen). The target CpGs were evaluated by converting the resulting pyrograms to numerical values for peak heights to calculate the percentage of methylation.

Statistical analysis. The chi square test was used to examine the statistical significance of a relationship between categorized variables. Nonparametric statistics were used to test continuous variables for differences between two subgroups (Wilcoxon Mann Whitney test). Quantitative DNA methylation data derived from MassARRAY were treated as continuous variables and missing measurements were imputed in multivariable regression analyses using samples with replacement from the non-missing values (single imputations). Linear associations between two continuous variables were quantified by Pearson correlation coefficient. *P* values <0.05 were considered to be statistically significant. The association between percentage of methylation and overall survival (OS), disease-free survival (DFS) and cumulative incidence of relapse (CIR) was assessed univariately for each CpG unit using a Cox proportional hazards regression model. The prognostic power of methylation at each CpG unit was expressed by the .632+ bootstrapped time-integrated Brier score measuring the prediction error (PE) of the model.¹² To build a

prognostic model for OS based on CpG methylation, the 127-case dataset was randomly divided into a training set (80 cases) and a validation set (47 cases), with both sets matched for distribution of patient age and follow-up periods. Prognostic models for DFS and CIR, applicable only to patients having received allogeneic hematopoietic stem cell transplantation (HSCT), were based on 97 cases (61 training and 36 validation cases). Prognostic signatures were developed using a L1 penalized Least Absolute Shrinkage and Selection Operator (LASSO) Cox regression model with incorporated variable selection, with the possibility of including all interrogated CpG units. Models for CIR were fitted by competing risks regression.¹³ The significance of the prognostic signatures was then verified in the validation set. The Kaplan-Meier method was used to estimate OS and DFS probabilities. Results were expressed as 5-year probability with 95% confidence interval (95% CI). The two-sided log-rank test was used to test the equality of survivorship functions in different subgroups. CIR curves correspond to the cause-specific hazards adjusted for competing risk, which is transplantation-related mortality (TRM).¹⁴⁻¹⁶ Gray's test was used to compare cumulative incidence curves. Statistical analysis was performed using the R statistical environment version 2.11.0 (with R packages rms v3.0-0, pec v1.1.1, peperr v1.1-5 penalized v0.9-31, cmprsk v2.2-1) and SPSS for Windows 17.0.

Results

We pre-screened the CpG island methylation status of 14 candidate genes in a cohort of 86 children with JMML and 15 normal controls, using a liquid chromatography-based method (msDHPLC) (Supplemental Figure S1). The candidate genes were selected based on hypermethylation previously documented in other types of cancer or leukemia (*CALCA*, *CDKN1C*, *CDKN2B*, *DAPK1*, *MGMT*,

MLH1, *RARB*, *RASSF1*, *SOCS1*, *TP73*), or based on involvement in the Ras signal transduction pathway, which has a prominent role in JMML pathogenesis (*BMP4*, *PAWR*, *RASA1*, *RECK*).¹⁷⁻¹⁹ Among these genes, four carried aberrant methylation as determined by msDHPLC: bone morphogenetic protein 4 (*BMP4*) in 28 of 86 JMML cases, calcitonin A (*CALCA*) (27/86 cases), cyclin-dependent kinase inhibitor 2B (*CDKN2B*) (17/86 cases) and retinoic acid receptor beta (*RARB*) (13/86 cases) (Supplemental Table S2). For the other 10 genes studied there was no evidence of aberrant CpG island methylation in 86 JMML cases. All 14 gene CpG islands exhibited normal methylation in 15 control samples obtained from healthy individuals.

We next employed MassARRAY technology to generate quantitative high-resolution CpG methylation patterns of the *BMP4*, *CALCA*, *CDKN2B*, and *RARB* genes in leukemic cells from an expanded cohort of 127 JMML cases which included the previous 86 cases (Figure 1). We found that the average levels of CpG methylation at the *BMP4* locus ranged from 0.9% to 56.1% in JMML but were 3.6%–12.1% in PB leukocytes from 15 normal individuals (Supplemental Table S3). *CALCA* methylation ranged from 1.3% to 92.9% in JMML and 5.6%–12.9% in the normal group (Supplemental Table S3). *CDKN2B* was methylated at 0.5% to 45.6% in JMML and 1.5%–6.2% in normals (Supplemental Table S3). *RARB* methylation ranged from 0.0% to 42.0% in JMML and 0.0%–8.8% in normal subjects (Supplemental Table S3). Based on the levels of methylation observed in normal controls, we regarded a CpG island as “hypermethylated” in a JMML sample if its average methylation across all CpGs measured was beyond three standard deviations from the mean observed in 15 normal individuals. Using this definition, 46/127 JMML cases (36%) exhibited *BMP4* hypermethylation, 69/127 JMML cases (54%) were hypermethylated at *CALCA*, 28/127 JMML cases (22%) had *CDKN2B* hypermethylation and 16/127

JMML cases (13%) showed aberrant *RARB* methylation (Figure 1). We tested whether the source material of leukemic cells (BM or PB specimens) had an influence on aberrant methylation and found no difference when paired BM/PB samples from the same patient were measured (Supplemental Figure S2). Similarly, there was no difference in methylation when granulocytes and mononuclear cells derived from the same clinical specimen were compared (Supplemental Figure S2).

We next asked whether hypermethylation at the four genetic loci correlated with specific clinical or hematologic features in JMML (Table 1). We found that hypermethylation at each of the 4 genes was strongly associated ($p < 0.001$) with older age at diagnosis. Elevated percentage of hemoglobin F (HbF) at diagnosis was associated with methylation at the *BMP4* and *CALCA* genes ($p = 0.008/0.004$). These observations seemed intriguing, as it is well documented that older age and high HbF percentage at diagnosis are strong predictors of treatment failure in JMML.^{6,20} The myeloblast count in the BM was associated with *CALCA* methylation ($p = 0.001$). A weaker association was seen between *CALCA* and *CDKN2B* hypermethylation and aberrant karyotype ($p = 0.010/0.023$). There was no correlation of aberrant CpG island methylation at any of the 4 loci with sex, leukocyte count, hemoglobin, monocyte count, blast percentage in PB, spleen size, or mutational JMML subtype (*NF1*, *PTPN11*, *KRAS/NRAS*, *CBL*) (Table 1).

The association of hypermethylation with known clinical risk factors suggested that the presence of hypermethylation at time of JMML diagnosis might be predictive of poor outcome. To test this possibility in an unsupervised and unbiased approach, we randomly selected a training set of 80 cases from the total 127-patient cohort. This set included 61 children who had received allogeneic HSCT and were thus considered as uniformly treated. The treatment in non-transplanted children was

heterogeneous and included supportive care alone, cytoreductive low-dose chemotherapy, high-intensity induction regimens, or more experimental agents. The remaining 47 cases (including 36 HSCT recipients) were used as validation set. Both sets were matched for distribution of methylation levels, patient age and follow-up periods (Supplemental Table S4 and Supplemental Figure S3). Each CpG unit was regarded as an individual disease marker regardless of genetic location and its predictive power was tested in a univariate Cox model for OS of the 80 training cases. In 61 patients who had received HSCT, the CpG units were also tested for influence on DFS and CIR. The prediction error of the models was controlled using a bootstrapping algorithm as detailed in the Methods section. We found that 8 of 53 CpG units had strong prognostic value for OS (defined as prediction error smaller than the Kaplan-Meier PE minus twice its standard error) and 18 of 53 CpG units had strong prognostic value for CIR. Ten of 53 CpG units had intermediate prognostic value for OS (PE < Kaplan-Meier PE minus one standard error) and 22 of 53 CpG units had intermediate prognostic value for CIR. Among the top 10 prognostic CpG units for OS, seven were located at the *BMP4* gene, one at *CDKN2B* and 2 at *RARB*.

Employing a LASSO Cox proportional hazards model, prognostic scores for OS were calculated from CpG methylation data using the training set of 80 cases and for DFS and CIR using 61 post-HSCT cases (Supplemental Table S4). The scores were then tested in the independent validation set of 47 patients, of whom 36 had received HSCT. We found that the CpG methylation score was still prognostic in the independent group of JMML patients for both OS ($p=0.016$; likelihood ratio test) and CIR ($p=0.049$). There was no prognostic value for DFS after HSCT ($p=0.431$), probably reflecting that TRM is a confounding variable which is unrelated to gene hypermethylation of leukemic cells at diagnosis.

Survival analyses showed that the probability of 5-year OS in 42 of 127 patients representing the lowest tertile of methylation scores was 0.72 (95% CI 0.56–0.88) whereas it was only 0.41 (95% CI 0.45–0.79) in 42 patients with methylation scores in the highest tertile ($p=0.002$, hazard ratio 3.51 [95% CI 1.61–7.65]) (Figure 2A). The probability of 5-year DFS among 97 transplanted patients was 0.63 (95% CI 0.46–0.81) in the lowest tertile of scores but was 0.30 (95% CI 0.14–0.47) in the highest tertile ($p=0.012$, hazard ratio 2.56 [95% CI 1.23–5.32]) (Figure 2B). The 5-year CIR among 97 transplanted patients was 0.10 (95% CI 0.03–0.29) for patients in the lowest score tertile but was 0.52 (95% CI 0.37–0.73) in the top tertile ($p=0.007$, hazard ratio 5.40 [95% CI 1.57–18.56]) (Figure 2C). Taken together, the results indicate that aberrant CpG island methylation in JMML has prognostic implications and predicts the risk of relapse after HSCT. The prognostic power of gene hypermethylation in JMML was reproducible also when the non-quantitative msDHPLC methodology was applied (Supplemental Figure S4). This suggests that msDHPLC can be useful for methylation assessment in clinical environments where MassARRAY equipment is not available.

To identify other prognostic variables in our series of JMML patients and evaluate the relative contribution of CpG methylation to prognosis, the clinical or hematologic parameters listed in Table 1 were tested in univariate analysis for influence on OS in the 80-patient training cohort. Consistent with previous reports on prognostic factors in JMML,^{6,20,21} age above 2 years was an adverse factor ($p=0.024$, hazard ratio 2.24 [95% CI 1.09–4.59]). Hemoglobin concentration at diagnosis (<10 g/dL) emerged as an additional factor ($p=0.017$, hazard ratio 2.87 [95% CI 1.17–7.05]). There was no prognostic value of white blood count, platelet count, blast percentage in BM or PB, monocyte percentage in BM or PB, splenomegaly,

cytogenetics or mutational subtype. To assess whether the prognostic power of the methylation phenotype was independent of age or hemoglobin concentration, these variables were entered in a multivariate Cox regression model for OS which was run on the independent 47-patient validation dataset. Only the presence of aberrant CpG island methylation at diagnosis retained prognostic power in multivariate analysis (Cox regression with backward selection; $p_{in} = 0.05$, $p_{out} = 0.10$). Likewise, when the same procedure was carried out for CIR as outcome endpoint, the methylation score emerged as sole independent prognostic factor. The score reached no significant level of prediction when tested for DFS. In summary, CpG island hypermethylation was identified as a robust marker of poor prognosis in JMML.

JMML is thought to arise in an early progenitor cell that retains the capability of differentiating into the erythroid, myeloid and monocytic lineages.²² To test whether aberrant methylation is specific to leukemic cell progeny in JMML, primary leukemic cells from spleens of two JMML patients with *BMP4* hypermethylation (D 360 and D 397 in Supplemental Tables S2 and S3) were flow-sorted into monocytes (CD14+), erythroid cells (CD235a+), progenitor cells (CD34+), T lymphocytes (CD3+) or B lymphocytes (CD19+). The leukemic cells of both patients were known to harbor somatically acquired *RAS* gene mutations (*KRAS* c.G35T in patient D 360; *NRAS* c.G38A in patient D 397). We found in both cases that CD14+ cells, CD235a+ cells and CD34+ cells contained the *RAS* mutation and exhibited increased *BMP4* methylation, whereas CD3+ and CD19+ cells carried wildtype *RAS* and had normal methylation (Figure 3). To quantify the degree of DNA methylation at the *BMP4*, *CALCA*, *CDKN2B* and *RARB* CpG islands in normal hematopoietic progenitor cells, we purified CD34+ cells from cord blood of three healthy newborns. Bisulfite sequencing revealed normal levels of methylation at each CpG island in all three

samples (data not shown). These results indicate that aberrant methylation is linked to leukemic hematopoiesis in JMML and can be traced back to the CD34+ progenitor cell compartment. The observation supports the concept that aberrant DNA methylation is clonal and associated with early pathogenetic events in JMML.

The common association of older age and increasing methylation with poor prognosis suggested that both features might reflect biologic properties of the underlying disease and, hence, that cases evolving toward refractory disease might be characterized by a higher degree of aberrant methylation. To test this hypothesis, we analyzed longitudinal samples from three patients at diagnosis, in remission after HSCT, at relapse and (if attained) in second remission (Table 2). In patient D003, the *RARB* CpG island was 2% methylated at diagnosis and progressed to 16% methylation at relapse, and *CALCA* methylation increased from 3% to 61% between diagnosis and relapse. Similarly, in patient D098 the methylation of *CALCA* had increased from 13% to 80% and that of *RARB* from 0% to 33% by the time of relapse. In patient D155, the degree of methylation was already substantial at diagnosis and did not progress further (Table 2). In summary, the observations indicate that some JMML cases acquire a higher methylated phenotype at relapse and support the idea that increasing DNA methylation parallels JMML evolution toward more aggressive disease.

Gene-specific DNA hypermethylation in malignant cells is often paralleled by genome-wide DNA hypomethylation, mainly affecting repetitive elements such as LINE1.²³ To test whether JMML cells were characterized also by global DNA hypomethylation, we used LINE1 bisulfite pyrosequencing²⁴ and assessed the methylation density of genomic LINE1 elements in 8 hypermethylated JMML samples, 8 JMML samples with normal methylation and 12 normal controls (Figure

4). Although we found no consistent difference in LINE1 methylation between hypermethylated and normally methylated JMML samples or between JMML cells and normal hematopoietic cells, it was interesting to note that 2 of 8 hypermethylated JMML cases but none of 8 JMML cases with normal methylation exhibited decreased LINE1 methylation (Figure 4).

To investigate the relation between CpG island methylation and gene silencing in JMML cells, the RNA expression of *BMP4*, *CALCA*, *CDKN2B* and *RARB* was interrogated by reverse-transcriptase PCR in JMML MNC and healthy blood cells (Figure 5A). *BMP4* was expressed at readily detectable levels in normal blood cells but was silent in JMML. *CALCA* transcripts were demonstrable neither in JMML nor controls. The *CDKN2B* and *RARB* genes were expressed in JMML and controls. It was noteworthy that the latter two genes were expressed at considerably lower levels in JMML (Figure 5A). We next performed quantitative reverse-transcriptase PCR measurements of *CDKN2B* and *RARB* expression in a series of JMML cases and compared the results to the level of CpG island methylation for each JMML sample. *RARB* expression was inversely correlated with methylation (Figure 5B), but no such correlation was seen for *CDKN2B*. It is tempting to speculate that *RARB* promoter methylation may contribute to the variable clinical response of JMML to isotretinoin.²⁵ We had no opportunity to test this hypothesis further, as none of the patients reported here had been treated with retinoids. Additional studies will be required to better understand the functional role and therapeutic implications of *RARB* promoter DNA methylation in JMML.

Discussion

It is widely recognized that aberrant DNA methylation is a hallmark of malignant disease, including MDS and MPN. However, data on DNA methylation in JMML has been scarce in the literature. In this study, we employed MassARRAY to analyze leukemic cells from 127 children with JMML for aberrant DNA methylation at four gene loci of interest (*BMP4*, *CALCA*, *CDKN2B*, and *RARB*), identified after prescreening 14 candidate genes. The 4 genes were hypermethylated in 13 to 54% of JMML cases. The BMP4 protein, a member of the TGF β -like family of growth factors,²⁶ participates in the initiation of hematopoietic gene expression and enhances hematopoietic differentiation.²⁷ The present report is the first to implicate hypermethylated *BMP4* in a hematologic disorder. The *CALCA* gene is a well-known target of aberrant methylation in chronic myeloid leukemia progressing to accelerated phase.²⁸ Those results and ours are consistent with the idea that *CALCA* methylation marks a more aggressive behavior of MPN.²⁸ Epigenetic dysregulation of the cell cycle inhibitor p15/INK4b, encoded by the *CDKN2B* gene, has been implicated in hematologic malignancy by numerous publications (reviewed in ref. 2). Specifically, our findings confirm and extend a previous study reporting *CDKN2B* hypermethylation in 3 of 18 JMML cases.⁷ *RARB* encodes the beta polypeptide of the nuclear retinoid acid receptor. A role for epigenetic repression of the retinoid acid signaling pathway in myeloid leukemogenesis was discussed.²⁹ Our data indicate that *RARB* is frequently underexpressed in JMML cells and suggest that aberrant *RARB* methylation may contribute to the silent state. Although based on a limited number of samples, these observations are compatible with the antiproliferative activity of retinoids in some JMML patients.^{25,30} We noted that the levels of methylation at the *BMP4*, *CDKN2B* and *RARB* CpG islands showed some correlation

within each case of JMML, whereas the association was less evident for *CALCA* methylation (Supplemental Table S3). The observation of common hypermethylation across different genes may suggest that some JMML cases are marked by a general CpG island methylator phenotype (CIMP).³¹ It will be required to complement our findings with genome-wide CpG methylation data to confirm the presence of a CIMP in JMML.

The most remarkable finding of the present study is the fact that gene hypermethylation at diagnosis was clearly associated with poor OS and a high risk of treatment failure due to relapse after HSCT. These findings establish DNA hypermethylation as a feature of an aggressive JMML variant which was previously not identifiable through molecular genetic parameters. While the precise target genes of methylation that contribute to the refractory phenotype remain unknown, it is interesting to note that an overall increase in gene-specific DNA methylation appears to characterize advanced or high-risk disease not only in JMML, but also in other malignant disorders of myelopoiesis, such as MDS, acute myeloid leukemia and chronic myeloid leukemia.³²⁻³⁴

Clinical and hematologic parameters with prognostic significance have been well established in JMML.^{6,20} Our results suggest that the assessment of DNA methylation at diagnosis may be useful for discriminating low-risk from high-risk JMML cases even within known clinical risk groups, most notably within the unfavorable age group of children above 2 years of age. This was also supported by a multivariate Cox model of clinical and hematologic parameters, from which DNA methylation emerged as an independent prognostic determinant. As a note of caution, these conclusions are based on retrospective analyses and prospective data are needed for further validation. A recent study found that patients with JMML could

be separated into two prognostic groups based on gene expression profiles.³⁵ Interestingly, the profile of JMML cells in cases with poor prognosis was reminiscent of acute myeloid leukemia,³⁵ consistent with our observation that such cases exhibit a higher methylation phenotype.

We have recently demonstrated that *CBL* mutations in JMML are of germline origin in most, if not all cases.³⁶ JMML with *CBL* mutation appears to have a peculiar clinical phenotype, characterized by a less aggressive course and a high rate of conversion to stable mixed chimerism after HSCT.³⁶ The mild course is in good agreement with the observations reported here, as *CBL*-positive cases tended to have normal DNA methylation (data not shown).

Some aspects with relevance to clinical practice emerged from the study. The EWOG-MDS recommends that every JMML patient should receive HSCT without unnecessary delay, because a parameter capable of identifying patients who would benefit from non-HSCT strategies has not yet been discovered.^{37,38} The differential methylation observed in JMML provides no immediate ground to change this policy, as the overall cure rate is far from satisfactory even in cases with normal DNA methylation. However, our data suggest that high-methylation cases may be good candidates for complementary approaches, for example pre-HSCT window therapies with DNA methyltransferase inhibitors³⁹ or novel strategies exploiting graft-versus-leukemia effects exerted by CD8+ regulatory T cells with specific anti-leukemia activity without simultaneous capacity of inducing graft-versus-host reaction.⁴⁰

Acknowledgments

This work was supported by Deutsche Forschungsgemeinschaft (Grant No. KR3473/1-1 to CF; Priority Program SPP1463 "Epigenetic Dysregulation in Myeloid

Neoplasia” to CP, CMN and CF), Deutsche Krebshilfe (Grant No. 108220 to CMN, CF), Deutsche José Carreras Leukämienstiftung (Grant No. R08/19 to CF), Sofia Luce Rebuffat Foundation (to FL), and Förderverein für krebskranke Kinder Freiburg e.V. The authors thank all collaborators of the European Working Group of Myelodysplastic Syndromes in Childhood for contributing clinical data and research material.

Disclosure of Conflicts of Interest

The authors declare no competing financial interests.

Authorship Contributions

C.F. designed research. C.O.B., A.R.P., P.N., R.C., I.S., T.W. and C.F. performed laboratory research. B.S., H.H., M.Ze., J.S., E.B., B.D.M., M.T., M.M.v.d.H., D.W., F.L., C.M.N. and C.F. provided study materials and treated patients. All authors collected and assembled experimental or clinical data. C.O.B., A.R.P., P.N., R.C., M.Zu., C.P., C.M.N. and C.F. analyzed and interpreted data. C.O.B. and C.F. wrote the manuscript, which was revised and approved by all co-authors.

References

1. Jones PA, Baylin SB. The fundamental role of epigenetic events in cancer. *Nat Rev Genet* 2002;3:415-428.
2. Boultonwood J, Wainscoat JS. Gene silencing by DNA methylation in haematological malignancies. *Br J Haematol* 2007;138:3-11.
3. Flotho C, Kratz CP, Niemeyer CM. Targeting RAS signaling pathways in juvenile myelomonocytic leukemia. *Curr Drug Targets* 2007;8:715-725.
4. Loh ML, Sakai DS, Flotho C, Kang M, Fliegau M, Archambeault S, et al. Mutations in CBL occur frequently in juvenile myelomonocytic leukemia. *Blood* 2009;114:1859-1863.
5. Steinemann D, Arning L, Praulich I, Stuhmann M, Hasle H, Stary J, et al. Mitotic recombination and compound-heterozygous mutations are predominant NF1-inactivating mechanisms in children with juvenile myelomonocytic leukemia and neurofibromatosis type 1. *Haematologica* 2010;95:320-323.
6. Niemeyer CM, Aricò M, Basso G, Biondi A, Cantù-Rajoldi A, Creutzig U, et al. Chronic myelomonocytic leukemia in childhood: a retrospective analysis of 110 cases. *Blood* 1997;89:3534-3543.
7. Hasegawa D, Manabe A, Kubota T, Kawasaki H, Hirose I, Ohtsuka Y, et al. Methylation status of the p15 and p16 genes in paediatric myelodysplastic syndrome and juvenile myelomonocytic leukaemia. *Br J Haematol* 2005;128:805-812.
8. Johan MF, Bowen DT, Frew ME, Goodeve AC, Reilly JT. Aberrant methylation of the negative regulators RASSF1A, SHP-1 and SOCS-1 in myelodysplastic syndromes and acute myeloid leukaemia. *Br J Haematol* 2005;129:60-65.
9. Liu YL, Castleberry RP, Emanuel PD. PTEN deficiency is a common defect in juvenile myelomonocytic leukemia. *Leuk Res* 2009;33:671-677.
10. Batz C, Sandrock I, Niemeyer CM, Flotho C. Methylation of the PTEN gene CpG island is infrequent in juvenile myelomonocytic leukemia. *Leuk Res* 2009;33:1578-1579.
11. Ehrich M, Nelson MR, Stanssens P, Zabeau M, Liloglou T, Xinarianos G, et al. Quantitative high-throughput analysis of DNA methylation patterns by base-specific cleavage and mass spectrometry. *Proc Natl Acad Sci U S A* 2005;102:15785-15790.
12. Graf E, Schmoor C, Sauerbrei W, Schumacher M. Assessment and comparison of prognostic classification schemes for survival data. *Stat Med* 1999;18:2529-2545.
13. Fine JP, Gray RJ. A proportional hazards model for the subdistribution of a competing risk. *J Am Stat Assoc* 1999;94:496-509.

14. Pepe MS, Longton G, Pettinger M, Mori M, Fisher LD, Storb R. Summarizing data on survival, relapse, and chronic graft-versus-host disease after bone marrow transplantation: motivation for and description of new methods. *Br J Haematol* 1993;83:602-607.
15. Gooley TA, Leisenring W, Crowley J, Storer BE. Estimation of failure probabilities in the presence of competing risks: new representations of old estimators. *Stat Med* 1999;18:695-706.
16. Klein JP, Rizzo JD, Zhang MJ, Keiding N. Statistical methods for the analysis and presentation of the results of bone marrow transplants. Part 2: Regression modeling. *Bone Marrow Transplant* 2001;28:1001-1011.
17. Ordway JM, Williams K, Curran T. Transcription repression in oncogenic transformation: common targets of epigenetic repression in cells transformed by Fos, Ras or Dnmt1. *Oncogene* 2004;23:3737-3748.
18. Pruitt K, Ulku AS, Frantz K, Rojas RJ, Muniz-Medina VM, Rangnekar VM, et al. Ras-mediated loss of the pro-apoptotic response protein Par-4 is mediated by DNA hypermethylation through Raf-independent and Raf-dependent signaling cascades in epithelial cells. *J Biol Chem* 2005;280:23363-23370.
19. Chang HC, Cho CY, Hung WC. Silencing of the metastasis suppressor RECK by RAS oncogene is mediated by DNA methyltransferase 3b-induced promoter methylation. *Cancer Res* 2006;66:8413-8420.
20. Locatelli F, Nöllke P, Zecca M, Korthof E, Lanino E, Peters C, et al. Hematopoietic stem cell transplantation (HSCT) in children with juvenile myelomonocytic leukemia (JMML): results of the EWOG-MDS/EBMT trial. *Blood* 2005;105:410-419.
21. Hasle H, Baumann I, Bergsträsser E, Fenu S, Fischer A, Kardos G, et al. The International Prognostic Scoring System (IPSS) for childhood myelodysplastic syndrome (MDS) and juvenile myelomonocytic leukemia (JMML). *Leukemia* 2004;18:2008-2014.
22. Flotho C, Valcamonica S, Mach-Pascual S, Schmahl G, Corral L, Ritterbach J, et al. RAS mutations and clonality analysis in children with juvenile myelomonocytic leukemia (JMML). *Leukemia* 1999;13:32-37.
23. Esteller M. Cancer epigenomics: DNA methylomes and histone-modification maps. *Nat Rev Genet* 2007;8:286-298.
24. Yang AS, Estecio MR, Doshi K, Kondo Y, Tajara EH, Issa JP. A simple method for estimating global DNA methylation using bisulfite PCR of repetitive DNA elements. *Nucleic Acids Res* 2004;32:e38.
25. Castleberry RP, Emanuel PD, Zuckerman KS, Cohn S, Strauss L, Byrd RL, et al. A pilot study of isotretinoin in the treatment of juvenile chronic myelogenous leukemia. *N Engl J Med* 1994;331:1680-1684.

26. Heldin CH, Miyazono K, ten Dijke P. TGF-beta signalling from cell membrane to nucleus through SMAD proteins. *Nature* 1997;390:465-471.
27. Pick M, Azzola L, Mossman A, Stanley EG, Elefanty AG. Differentiation of human embryonic stem cells in serum-free medium reveals distinct roles for bone morphogenetic protein 4, vascular endothelial growth factor, stem cell factor, and fibroblast growth factor 2 in hematopoiesis. *Stem Cells* 2007;25:2206-2214.
28. Nelkin BD, Przepiorka D, Burke PJ, Thomas ED, Baylin SB. Abnormal methylation of the calcitonin gene marks progression of chronic myelogenous leukemia. *Blood* 1991;77:2431-2434.
29. Fazi F, Zardo G, Gelmetti V, Travaglini L, Ciolfi A, Di Croce L, et al. Heterochromatin gene repression of the retinoic acid pathway in acute myeloid leukemia. *Blood* 2007;109:4432-4440.
30. Muccio DD, Brouillette WJ, Breitman TR, Taimi M, Emanuel PD, Zhang X, et al. Conformationally defined retinoic acid analogues. 4. Potential new agents for acute promyelocytic and juvenile myelomonocytic leukemias. *J Med Chem* 1998;41:1679-1687.
31. Issa JP. CpG island methylator phenotype in cancer. *Nat Rev Cancer* 2004;4:988-993.
32. Nagy E, Beck Z, Kiss A, Csoma E, Telek B, Konya J, et al. Frequent methylation of p16INK4A and p14ARF genes implicated in the evolution of chronic myeloid leukaemia from its chronic to accelerated phase. *Eur J Cancer* 2003;39:2298-2305.
33. Jiang Y, Dunbar A, Gondek LP, Mohan S, Rataul M, O'Keefe C, et al. Aberrant DNA methylation is a dominant mechanism in MDS progression to AML. *Blood* 2009;113:1315-1325.
34. Bullinger L, Ehrich M, Döhner K, Schlenk RF, Döhner H, Nelson MR, et al. Quantitative DNA methylation predicts survival in adult acute myeloid leukemia. *Blood* 2010;115:636-642.
35. Bresolin S, Zecca M, Flotho C, Trentin L, Zangrando A, Sainati L, et al. Gene expression-based classification as an independent predictor of clinical outcome in juvenile myelomonocytic leukemia. *J Clin Oncol* 2010;28:1919-1927.
36. Niemeyer CM, Kang MW, Shin DH, Furlan I, Erlacher M, Bunin NJ, et al. Germline CBL mutations cause developmental abnormalities and predispose to juvenile myelomonocytic leukemia. *Nat Genet* 2010;42:794-800.
37. Bergstraesser E, Hasle H, Rogge T, Fischer A, Zimmermann M, Noellke P, et al. Non-hematopoietic stem cell transplantation treatment of juvenile myelomonocytic leukemia: a retrospective analysis and definition of response criteria. *Pediatr Blood Cancer* 2007;49:629-633.
38. Flotho C, Kratz CP, Bergstraesser E, Hasle H, Stary J, Trebo M, et al. Genotype-phenotype correlation in cases of juvenile myelomonocytic leukemia with clonal RAS mutations. *Blood* 2008;111:966-967.

39. Furlan I, Batz C, Flotho C, Mohr B, Lübbert M, Suttorp M, et al. Intriguing response to azacitidine in a patient with juvenile myelomonocytic leukemia and monosomy 7. *Blood* 2009;113:2867-2868.

40. Locatelli F. Tolerance: pregnancy matters. *Blood* 2009;114:2208-2209.

	Total cohort	Normal <i>BMP4</i> methylation	<i>BMP4</i> hyper- methylation	<i>p</i>	Normal <i>CALCA</i> methylation	<i>CALCA</i> hyper- methylation	<i>p</i>	Normal <i>CDKN2B</i> methylation	<i>CDKN2B</i> hyper- methylation	<i>p</i>	Normal <i>RARB</i> methylation	<i>RARB</i> hyper- methylation	<i>p</i>
Hemoglobin F (age-adjusted)				0.008			0.004			0.172			0.176
Normal	24 (25%)	20 (35%)	4 (10%)		17 (71%)	7 (29%)		21 (28%)	3 (14%)		23 (27%)	1 (8%)	
Elevated	73 (75%)	38 (65%)	35 (90%)		26 (36%)	46 (64%)		54 (72%)	19 (86%)		61 (73%)	12 (92%)	
Missing	30												
Karyotype				1.000			0.010			0.023			0.226
Normal	86 (71%)	55 (71%)	31 (71%)		46 (82%)	39 (60%)		74 (75%)	12 (50%)		73 (68%)	13 (87%)	
Aberrant	36 (29%)	23 (29%)	13 (29%)		10 (18%)	26 (40%)		24 (25%)	12 (50%)		34 (32%)	2 (13%)	
Missing	5												
DNA source				0.854			1.000			0.138			0.598
PB	57	37 (46%)	20 (44%)		26 (45%)	31 (46%)		48 (49%)	9 (32%)		51 (46%)	6 (38%)	
BM	70	44 (54%)	26 (56%)		32 (55%)	37 (54%)		51 (52%)	19 (68%)		60 (54%)	10 (62%)	
Mutation				0.076			0.320			0.778			0.411
<i>NF1</i>	16 (13%)	9 (11%)	7 (15%)	0.417	5 (9%)	11 (17%)	0.192	12 (12%)	4 (15%)	0.529	14 (13%)	2 (12%)	0.449
<i>PTPN11</i>	48 (38%)	26 (32%)	22 (49%)	0.089	19 (33%)	29 (43%)	0.150	36 (37%)	12 (44%)	0.391	39 (35%)	9 (56%)	0.174
<i>KRAS/NRAS</i>	30 (23%)	22 (27%)	8 (18%)	0.395	16 (28%)	14 (21%)	0.536	25 (25%)	5 (19%)	0.806	29 (26%)	1 (6%)	0.116
<i>CBL</i>	16 (13%)	13 (16%)	3 (7%)	0.126	9 (15%)	7 (10%)	0.290	14 (14%)	2 (7%)	0.406	14 (13%)	2 (13%)	0.855
No mutation	16 (13%)	11 (14%)	5 (11%)		9 (15%)	6 (9%)		12 (12%)	4 (15%)		14 (13%)	2 (13%)	
Missing	1												
Survival				0.001			0.240			0.505			0.006
Alive	81(64%)	61 (75%)	20 (44%)		40 (69%)	40(59%)		65 (66%)	16 (57%)		76 (69%)	5 (31%)	
Dead	46 (36%)	20 (25%)	26 (56%)		18 (31%)	28 (41%)		34 (34%)	12 (43%)		35 (31%)	11 (69%)	
Alive after HSCT				0.079			0.832			0.799			0.094
Yes	63 (66%)	45 (71%)	18 (53%)		30 (67%)	33 (64%)		50 (66%)	13 (62%)		59 (68%)	4 (40%)	
No	34 (34)	18 (29%)	16 (47%)		15 (33%)	19 (36%)		26 (34%)	8 (38%)		28 (32%)	6 (60%)	
No HSCT													
Relapse after HSCT				<0.001			0.070			0.265			0.021
Yes	26 (27%)	9 (14%)	17 (50%)		37 (82%)	34 (65%)		18 (24%)	8 (38%)		20 (23%)	6 (60%)	
No	71 (73%)	54 (86%)	17 (50%)		8 (18%)	18 (35%)		58 (76%)	13 (62%)		67 (77%)	4 (40%)	

Table 1. Clinical and hematologic characteristics at diagnosis and outcome of 127 children with JMML according to CpG island methylation at four genetic loci (*BMP4*, *CALCA*, *CDKN2B*, *RARB*). Hypermethylation was defined as a level of methylation exceeding 3 standard deviations from the mean observed in 15 healthy control individuals. For categorical variables, column percentages add to 100%. For continuous variables, median values and range are given. *P* values for significance of associations are based on chi square test for categorical variables and Wilcoxon Mann Whitney test for continuous variables. PB, peripheral blood; BM, bone marrow; HSCT, hematopoietic stem cell transplantation..

Table 2

Patient ID	Gene	Time point during clinical course				Age at diagnosis (months)	Age at relapse (months)
		At diagnosis	In remission after 1st HSCT	At relapse	In remission after 2nd HSCT		
D 155	<i>BMP4</i>	31%	n/a	28%	7%	63	75
	<i>CALCA</i>	32%	n/a	45%	4%		
	<i>CDKN2B</i>	46%	n/a	38%	3%		
	<i>RARB</i>	11%	n/a	10%	0%		
D 003	<i>BMP4</i>	7%	12%	18%	—	4	49
	<i>CALCA</i>	3%	5%	61%	—		
	<i>CDKN2B</i>	1%	2%	4%	—		
	<i>RARB</i>	2%	0%	16%	—		
D 098	<i>BMP4</i>	13%	n/a	8%	—	7	42
	<i>CALCA</i>	13%	n/a	80%	—		
	<i>CDKN2B</i>	4%	n/a	2%	—		
	<i>RARB</i>	0%	n/a	33%	—		

Table 2. Progression of aberrant methylation over time in three JMML patients. n/a, material not available.

Figure Legends

Figure 1. Quantitative DNA methylation analysis of *BMP4*, *CALCA*, *CDKN2B* and *RARB* CpG islands using MassARRAY in 127 JMML samples and 15 normal peripheral blood samples. Each row represents a sample and each column represents a CpG unit, which is a single CpG site or a combination of CpG sites. The position of the amplified sequence relative to the transcription start site is indicated above each color plot. The data are colour-coded according to degree of methylation (light green, 0%; dark blue, 100%; gray, no data). Next to each color plot, the DNA methylation levels are displayed as box plots in three categories: normal controls, JMML with normal methylation, and JMML with hypermethylation (exceeding the mean level of methylation in normal controls by more than three standard deviations).

Figure 2. Outcome of 127 JMML patients according to prognostic methylation score divided into tertiles. **(A)** Probability of survival from diagnosis, irrespective of disease status. Patients alive at last follow-up were censored. Death was considered as event. Numbers indicate the probability of 5-year survival and the 95% confidence interval (CI). **(B)** Probability of disease-free survival (DFS) after hematopoietic stem cell transplantation (HSCT) of 97 JMML patients who had received HSCT. Numbers indicate the probability of 5-year DFS and the 95% CI. DFS was defined as the probability of being alive and disease-free. Patients alive and disease-free at last follow-up were censored. Death and relapse were considered as events. **(C)** Cumulative incidence of relapse after HSCT of 97 patients who had received HSCT. Numbers indicate the 5-year cumulative incidence of relapse and the 95% CI.

Relapse incidence was defined as the probability of JMML relapse at a given time. Death without relapse was considered a competing event.

Figure 3. Lineage specificity of aberrant methylation in JMML patient D360. Hypermethylation of the *BMP4* CpG island was analyzed by msDHPLC and bisulfite sequencing in flow-sorted CD14+, CD34+, CD235a+, CD3+ and CD19+ spleen cell fractions. msDHPLC chromatograms (left): dotted lines represent normal control DNA; black lines, methylated control DNA; red lines, sample DNA. Bisulfite sequencing (center): horizontal lines represent individual alleles (4 per cell sample); filled circles, methylated cytosines; open circles, unmethylated cytosines. Genomic sequencing (right): The arrow indicates the position of the heterozygous *KRAS* c. 35 G>T mutation.

Figure 4. Quantitative LINE1 bisulfite pyrosequencing. **(A)** Example of LINE1 pyrogram. Percent proportions of C and T (corresponding to methylated and unmethylated cytosine) are shown in boxes above each CpG site (grey shade). Overall LINE1 methylation is estimated from the average proportion of C across 4 CpG sites. **(B)** LINE1 methylation at 4 CpG sites in hematopoietic cells from 12 normal controls and 21 JMML cases. The JMML cases are grouped into 8 cases with normal CpG island methylation (A054, CH017, D097, D116, D257, D454, D675, SC102) and 8 cases with hypermethylation in at least 3 of 4 CpG islands (D020, D127, D360, D361, D397, D567, D684, PL019).

Figure 5. Relationship of gene silencing and CpG island hypermethylation in JMML. **(A)** Reverse-transcriptase PCR to detect the mRNA expression of *BMP4*, *CALCA*,

CDKN2B and *RARB* in peripheral blood cells from 4 JMML patients (D360, D359, D651, D341) and 3 healthy individuals (N1, N11, N13). **(B)** mRNA expression levels of the *RARB* gene (left; N=33) and the *CDKN2B* gene (right; N=13) in JMML peripheral blood mononuclear cells in relation to CpG island methylation. Expression levels were measured by quantitative reverse-transcriptase PCR and CpG methylation was measured by MassARRAY. The average *RARB* mRNA expression in blood cells from 5 healthy individuals was used as calibrator and set to 1.0.

Figure 1

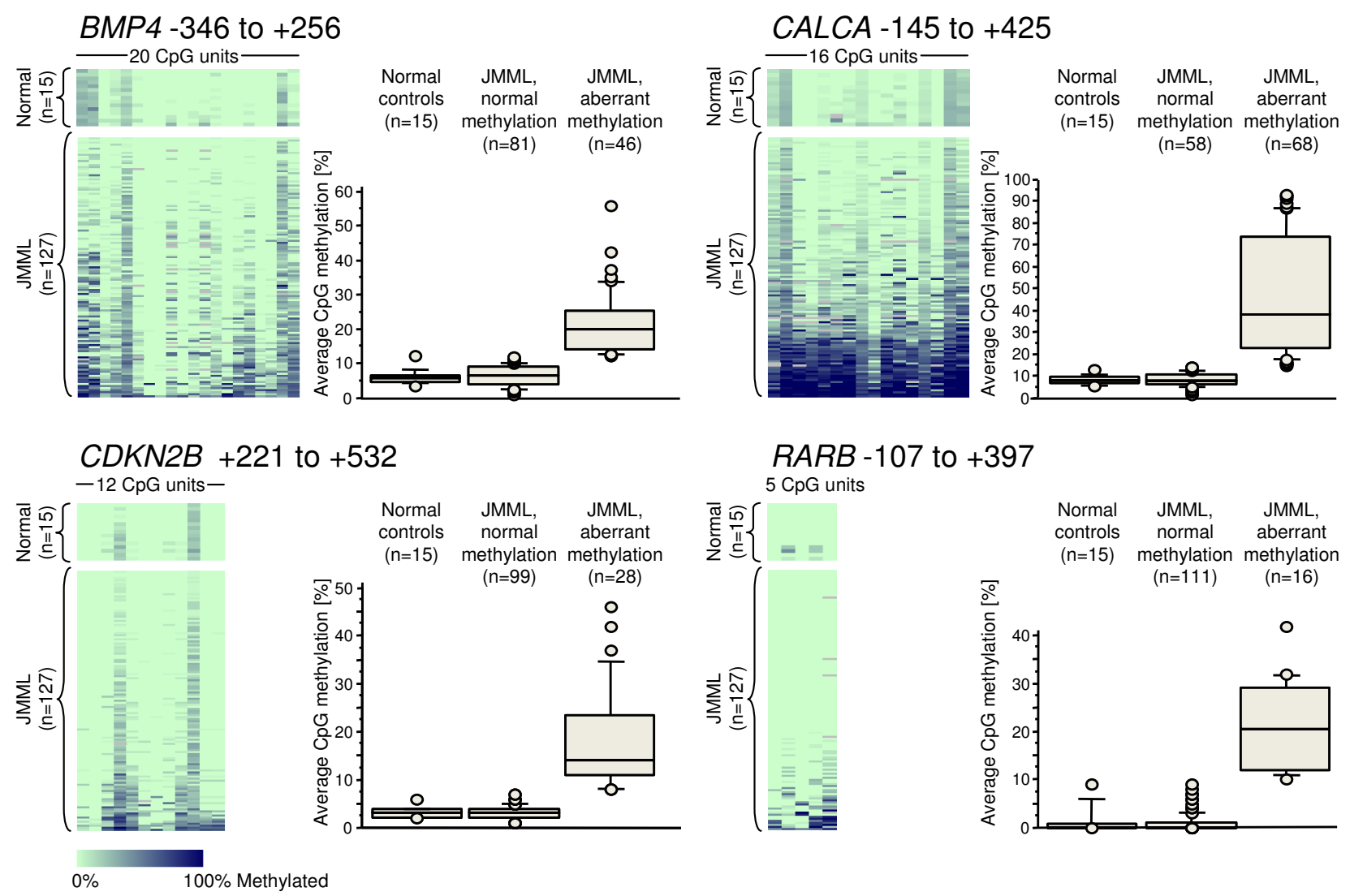
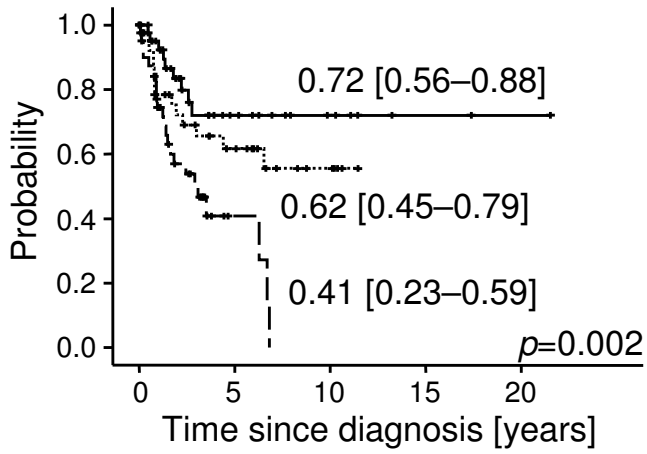


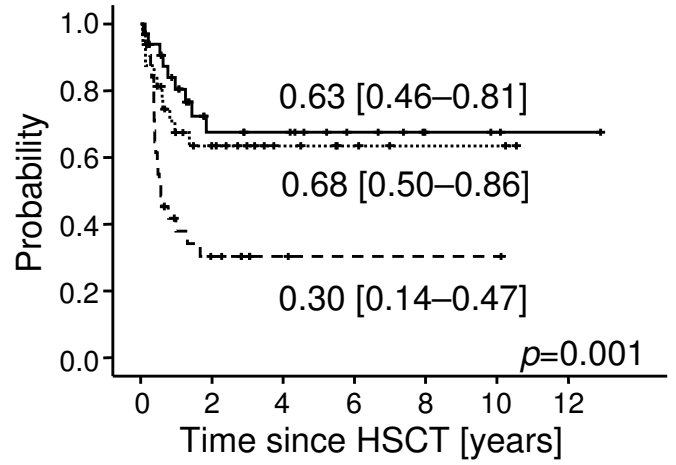
Figure 2

A Overall survival from diagnosis



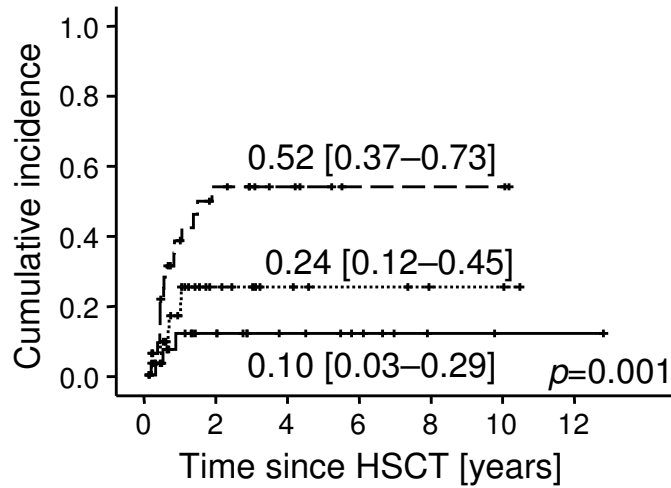
Score Tertile	Number of patients
Lowest —	42 13 6 2 1
Middle ···	43 15 5 0 0
Highest - -	42 3 0 0 0

B Disease-free survival after HSCT



Score Tertile	Number of patients
Lowest —	32 14 7 4 2 2 0
Middle ···	33 14 12 7 3 2 1
Highest - -	32 7 2 1 1 1 0

C Relapse after HSCT



Score Tertile	Number of patients
Lowest —	32 16 10 7 3 2 2
Middle ···	33 12 7 5 4 3 1
Highest - -	32 13 7 3 3 3 1

Figure 3

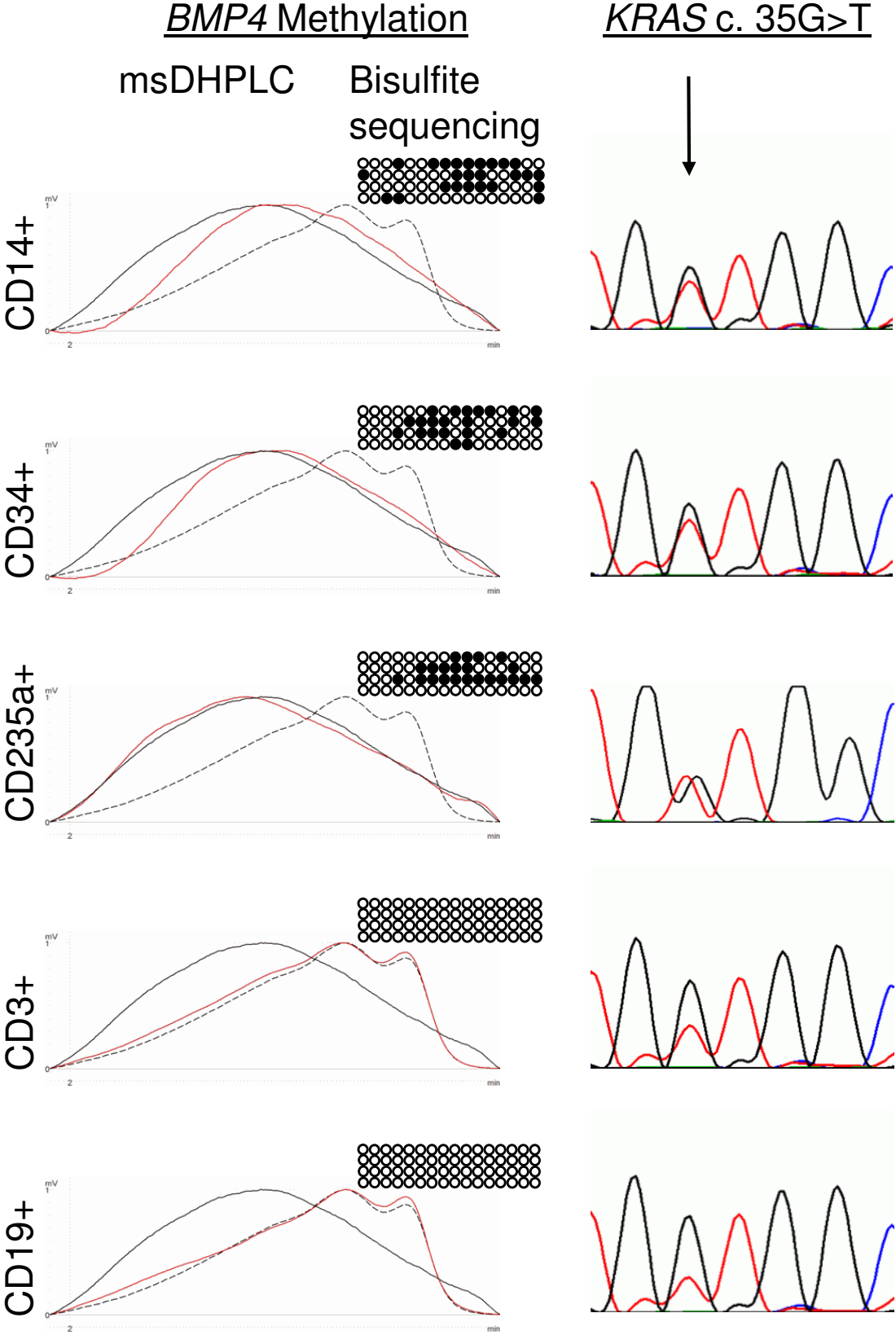


Figure 4

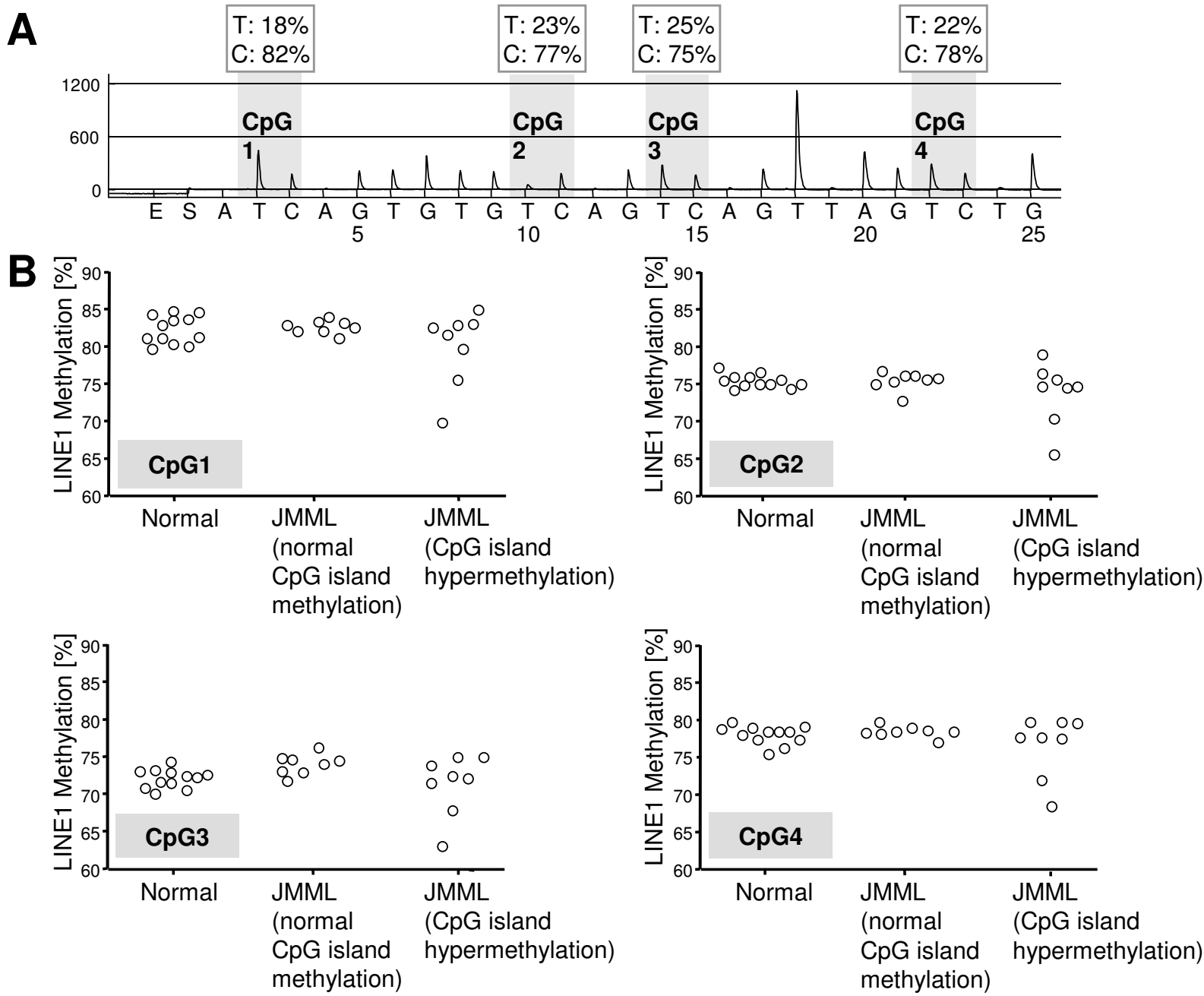


Figure 5

